Published in final edited form as:
Biochim Biophys Acta. 2004 April 12; 1655(0): 140–148. doi:10.1016/j.bbabio.2003.07.004.

The water-oxidation complex in photosynthesis

Kenneth Sauer[a,b,*] and **Vittal K. Yachandra**[a,*]

[a]Melvin Calvin Laboratory, Physical Biosciences Division, Lawrence Berkeley National Laboratory, Berkeley, CA, 94720, USA

[b]Lawrence Berkeley National Laboratory, Department of Chemistry, University of California, One Cyclotron Road, Berkeley, CA, 94720-5230, USA

Abstract

Studies of the photosynthetic water-oxidation complex of photosystem II (PS II) using spectroscopic techniques have characterized not only important structural features, but also changes that occur in oxidation state of the Mn_4 cluster and in its internal organization during the accumulation of oxidizing equivalents leading to O_2 formation. Combining this spectroscopic information with that from the recently published relatively low-resolution X-ray diffraction studies, we have succeeded in limiting the range of likely cluster arrangements. This evidence strongly supports several options proposed earlier by DeRose et al. [J. Am. Chem. Soc. 116 (1994) 5239] and these can be further narrowed using compatibility with electron paramagnetic resonance (EPR) data.

Keywords

Photosystem II; Oxygen-evolving complex; EXAFS; XANES; EPR; S-state; Oxygen evolution

1. Introduction

Our understanding of the mechanism of photosynthetic water oxidation by photosystem II (PS II) has been greatly aided by a variety of spectroscopic studies during more than 50 years [2–4]. At the time Jerry Babcock came to Berkeley in 1968, results based on rapid-transient optical spectroscopy and electron paramagnetic resonance (EPR) had proved valuable in elucidating the initial electron transfer events in PS I and in non-oxygen evolving photosynthetic bacteria. Exploration of PS II was less advanced, obscured in part by the behavior of an enigmatic EPR observation known as Signal II. Unlike Signal I, which arises from the oxidized primary electron donor $P700^+$ associated with PS I, Signal II exhibited complex kinetics that were not compatible with a similar assignment to $P680^+$ in PS II [5,6]. Jerry began to investigate this problem for his PhD thesis and continued to work on it during his subsequent career until he brought it to its current state of being largely understood. In the process he made use of and helped to develop increasingly sophisticated experimental tools to attack the problem.

*Corresponding authors. Tel.: +1-510-486-4330/4334; fax: +1-510-486-6059. KHSauer@LBL.GOV (K. Sauer), VKYachandra@LBL.GOV (V.K. Yachandra).

2. Jerry Babcock's early contributions to PS II research

In his initial studies at Berkeley, Jerry used polaro-graphic O_2 detection with a bare platinum electrode to explore the period 4 behavior of flash-induced O_2 formation in chloroplasts, expanding on earlier work by Joliot et al. [7] and Kok et al. [8] that had led to the formulation of the S-state cycle. Jerry's initial studies identified a 400-μs onset time for the formation of intermediate water-oxidation species, which he also showed had lifetimes of many seconds. These results appeared in his PhD thesis published just 30 years ago [9] and in two published articles. His first investigations using EPR were on dark-adapted intact chloroplasts, discovering a rise time of 1 s for flash-induced Signal II (slow) formation [10]. He showed that there were two different spectroscopic line shapes and partially resolved hyperfine structures that could be reversibly interconverted by changing ionic strength [11]. Signal II (slow) was photo-induced with high quantum yield and was present in roughly stoichiometric amounts with Signal I. Its behavior was suggestive of participation in one-time slow electron transfer to the S_2 and S_3 states on the water side of PS II.

During his PhD thesis research and during one subsequent postdoctoral year at Berkeley, he generated and collaborated in research that resulted in additional seven publications. He discovered a transient form of Signal II with fast decay kinetics in chloroplasts that had been inhibited in O_2 evolution, again in a 1:1 ratio with Signal I [12]. Redox studies showed that this species, Signal II (fast), has electron transfer properties consistent with those of the physiological donor to $P680^+$ [13]. Further studies using an inhibitor of O_2 evolution on the acceptor side showed that this inhibition could be relieved by oxidizing a PS II component with a one-electron midpoint potential of + 480 mV, although the chemical nature of this component was not known at that time, it has since been identified as the iron of the iron-quinone acceptor complex [14]. In another study, Jerry showed that there are two paths by which electron donors can gain access to PS II—one through the physiological donor and one that bypasses it [15]. Jerry returned to this fast-decaying Signal II after he arrived at Michigan State by sending his graduate student Bill Buttner to work with Mike Boska in our lab at Berkeley to show that the decay kinetics of the fast Signal II correlated under a variety of pH conditions with the re-reduction of $P680^+$ [16]. This verified the assignment of Signal II (fast) to the immediate electron donor to P680. Bob Blankenship and Jerry, while he was still at Berkeley, showed that reactivation of O_2 evolution capability restored the period 4 behavior in flash trains and eliminated the fast-decaying Signal II 5 [17]. Research with Art Ley showed periodicity of four flashes also in the green alga *Chlorella pyrenoidosis* and in the cyanobacterium *Anacystis nidulans* [18]. In a study on untreated chloroplasts using fast time-resolved EPR together with Bob Blankenship and Joe Warden, a very fast (500 μs) relaxing form of Signal II was observed [19]. Using instrumentation with ever faster detection and multiple signal averaging, Jerry and Bob were able to resolve the decay of Signal II (very fast) following individual flashes in a train and demonstrated that the kinetics becomes slower as the charge on the water-oxidation complex increases from S_1 through S_3 [20].

Of course, this story did not end when Jerry left Berkeley. When he returned to photosynthesis research at Michigan State, the question of the chemical identity of the species responsible for Signal II (slow) and Signal II (fast) or II (very fast) remained unresolved. They had been labeled with various letters of the alphabet, typically different in Europe and in America, and attempts to show that they were quinones of one sort or another encountered a stoichiometric insufficiency. In characteristic fashion Jerry followed a lead from EPR studies of an intermediate in ribonucleotide reductase activity and, in now classic studies done with Bridgette Barry, Rick Debus and Lee McIntosh, proved that two tyrosine side chains of the reaction center proteins D1 and D2 were responsible for what are now known as Y_Z and Y_D [21–23]. Thus, the tyrosyl radical of Y_Z is the immediate donor to

$P680^+$ and is responsible for Signal II (very fast) in intact chloroplasts and Signal II (fast) in inactivated preparations. The tyrosyl of Y_D is responsible for Signal II (slow) and reflects a light-sensitive redox-active toggle of still unknown function. This important clarification of the phenomena characteristically took Jerry into new realms of research involving ENDOR spectroscopy and molecular biology. Always the adventurer and never deterred by uncharted territory, he taught us many lessons during his too short life.

3. The water-oxidation enzyme

The redox-active center of the photosynthetic water-oxidation enzyme responsible for the S-states of PS II consists of a cluster of four Mn atoms, one Ca and one Cl [24–27]. Spectroscopic studies, using EPR and X-ray absorption spectroscopy (XAS) provide unambiguous evidence that the four Mn atoms are closely coupled, involving Mn–Mn distances of 2.7–3.4 Å [26,28]. Furthermore, the Ca atom also lies within this distance range of the Mn atoms, and some evidence supports the view that Cl^- is a ligand to Mn. Both EPR and XAS have been used to study the properties of the metal center in each of the isolatable S-states—S_0, S_1, S_2 and S_3. These studies show that the oxidation state of one or more Mn atoms changes in the $S_0 \rightarrow S_1$ and $S_1 \rightarrow S_2$ transitions, but apparently not in $S_2 \rightarrow S_3$ [29,30]. A current elaboration of the Kok cycle is shown in Fig. 1. While the structures of S_1 and S_2, based on extended X-ray fine structure (EXAFS) measurements, are essentially indistinguishable [1], those of S_0 and S_3 are distinctly different [29,31]. These differences are thought to reflect chemical changes associated with removing protons from water molecules and in the formation of the O–O bond, respectively.

Recent X-ray diffraction measurements have led to a preliminary relatively low resolution (3.7 Å) structure of the PS II complex from thermophilic cyanobacteria [32,33]. The Mn cluster has been located within this large (300 kDa) protein complex, and its electron density has been described as somewhat elongated (pear-shaped) in one direction and with all four Mn atoms lying nearly in a plane. Using studies of Mn-containing model compounds and ideas derived from knowledge of the structures of common Mn oxide minerals [34], we are able to reconcile the available information with a rather specific proposed Mn cluster geometry. This provides a basis for new and ongoing spectroscopic investigations, both on conventional PS II preparations and on single crystals. The insights arising from studies of oriented samples using polarized XAS are proving helpful in testing the proposed geometry.

4. Mn oxidation during S-state transitions

4.1. EPR evidence

The first direct measure of an individual S-state was the multiline EPR signal (MLR) reported by Dismukes and Siderer [35]. Analysis of this signal established that S_2 contains an odd number of electrons in the active center and that the unpaired electron(s) couple directly to Mn nuclei [35,36]. Further studies showed that the hyperfine structure is best explained by coupling to four Mn [37,38]. Subsequently, EPR signals were found to be associated with the S_0 [39,40] and the S_1 [41,42] states as well, but these are not so easily detected in untreated samples or by conventional EPR spectroscopy. Alterations of the PS II preparations in ways that halted the progress towards O_2 evolution produced additional EPR signals, one of which is associated with a nonviable S_3 state, identified as $S_2Y_Z\bullet$ [43,44]. Parallel polarization EPR signal s have also been reported from the S_3 state [45].

Related EPR studies focussed on other components of the PS II reaction center complex. We have seen that Jerry Babcock's earliest reported measurements were later shown to result from the tyrosine, Y_Z, responsible for transferring electrons to $P680^+$ from the Mn_4 complex, and from tyrosine Y_D. Direct evidence of charge separation in the PS II reaction

center was seen in a radical-pair polarized EPR signal that decayed rapidly once it was formed [46]. Oxidized cytochrome b_{559} also shows a characteristic EPR with a pronounced dependence on directionality in oriented membrane preparations. Y_D also shows a distinctive change in line shape with orientation, owing to anisotropy of the spin tensor. These orientation-dependent signals proved to be valuable in determining the degree of ordering (mosaic spread) in samples used for X-ray dichroism measurements, as described below [47].

4.2. X-ray absorption near edge structure (XANES) and Kβ XES evidence

The ability to detect small concentrations of transition metals present in metallo-enzyme systems was enabled by the development of X-ray fluorescence excitation spectroscopy by Jaklevic et al. [48]. This element-specific methodology enables one to look at properties of Mn, for example, without major interference from other elements, including other transition metals that are present in many multi-enzyme complexes such as PS II. The XAS spectra are delicately sensitive to the oxidation states and coordination geometries of the elements investigated; with the advent of higher quality data through technical improvements, subtle changes in the spectra of Mn in the different S-states have been characterized. Using series of single-turnover flashes and using the multiline EPR to characterize the samples, it has been possible to extract XANES spectra of each of the four stable S-states [30,49]. These spectra provide clear evidence of the participation of Mn in storing oxidizing equivalents during the $S_0 \rightarrow S_1$ and $S_1 \rightarrow S_2$ transitions, but did not support a similar involvement of Mn in the $S_2 \rightarrow S_3$ transition (see Fig. 1 for oxidation state assignments). Difficulties in interpreting what was happening in forming S_3 were subsequently resolved using the less ambiguous methodology of Kβ X-ray emission spectroscopy (XES), which showed more clearly the absence of Mn oxidation during $S_2 \rightarrow S_3$ [30]. Nevertheless, it is difficult at present to interpret the XANES spectra for this problem in more than an empirical fashion, owing to the difficulty of applying the relevant theory to a metal cluster where the local structure and chemical environment are largely unspecified.

5. Geometry of the metal cluster from EXAFS studies

EXAFS results from the backscattering of departing 1s electrons of Mn from neighboring atoms. The spectra are exquisitely sensitive to the distance of separation of the scattering atoms from the X-ray-excited atom, out to about 4 Å, and to the nature (atomic number) of the scattering atom. To interpret the results in terms of the coordination environment of the Mn, it has been necessary to examine a number of inorganic complexes of known structure, generously provided to us by our collaborators. On the basis of the latest findings, we conclude that each Mn is surrounded by a first coordination shell of O or N atoms at 1.8 to 2.0 Å, a set of Mn atoms at 2.7 Å and additional Mn at 3.3 Å [26]. Furthermore, studies using Sr to replace Ca [50] and, subsequently, direct measurements using Ca EXAFS [51], show unambiguously the presence of a 3.4-Å Mn–Ca vector. (The use of vector terminology to describe these inter-atomic interactions is particularly appropriate because of the direction information available from dichroism measurements on oriented samples.) Using model-compound data, it was straightforward to assign the 2.7-Å Mn–Mn vector to di-μ-oxo bridges between pairs of Mn atoms and the 3.3-Å Mn–Mn vector to a mono-μ-oxo bridged or similar longer interaction.

The separate contribution of individual S-states to the EXAFS was extracted using single-turnover flashes and deconvolution of the S-state using EPR, as mentioned above. The results show that the coordination environment of the Mn atoms is scarcely changed in going from the S_1 to the S_2 state [1]. Both the S_0 and the S_3 states do show structural changes, albeit not necessarily large ones. There is importantly a significant separation and increase of vector lengths in the 2.7-Å region. Dichroism measurements on oriented PS II

membranes [52] combined with careful quantitation lead to the conclusion that there are three Mn–Mn vectors of 2.7 Å length in S_1 and S_2, and that one of the three is lengthened to 2.85 Å in the S_0 state [31]. A similar loss of degeneracy in vector length occurs in the S_3 state [29]. The dichroism studies also provide information concerning the orientation of these vectors relative to the membrane normal, as well as for the Sr–Mn vectors in samples where Sr has been introduced in place of Ca [53]. Ongoing studies of the EXAFS of oriented single crystals of PS II in collaboration with the Berlin group should provide additional constraints on the geometrical arrangement of the metal atoms.

The relative numbers and orientation of these vectors already provide criteria for deciding among acceptable cluster geometries (see Fig. 2). The evidence supporting three 2.7-Å Mn–Mn vectors and one or two 3.3-Å Mn–Mn vectors coupled with one or two 3.4-Å Ca–Mn vectors serves to provide a basis for arguments against some previously proposed models, such as the cubane [54] or distorted cubane and the dimer-of-dimers model [26,55], which our group used as a working model for a number of years, although we always emphasized that it was one of the five (options A, E, F, G, and K, nomenclature as in Ref. [1]) of the 11 topologies that were favored by EXAFS data.

6. Cluster models

6.1. MnO_2 minerals

A proposal originally put forward by Russell and Hall [56] speculates that in PS II the MnO cluster and associated Ca had its evolutionary origin in the capture of Mn oxide precipitates in the early ocean by a non-oxygen evolving photosynthetic precursor microorganism. A likely source of the Mn, along with Fe and other transition elements, is thermal vents on the ocean floor and elsewhere, as witnessed today in the black smokers often associated with the boundaries of tectonic plates. Mn-rich nodules on the ocean floor and Mn-containing minerals composing rocks and soils provide abundant evidence for the widespread distribution of Mn. Furthermore, analysis of the published structures of many of these Mn-rich minerals shows evidence of the presence of oxygen-bridged Mn networks. In particular, a class of minerals designated tunnel-type MnO_2 minerals (hollandite is an example) exhibit both 2.7- and 3.3-Å Mn–Mn vectors in EXAFS measurements. On the basis of X-ray crystallography, it is possible to identify an assortment of geometries encompassing four Mn atoms linked by O-atom bridges within the crystal lattice [34]. A small subset of these possess the indicated three 2.7-Å and one or two 3.3-Å Mn–Mn vectors per four Mn (Fig. 3).

Another feature of the MnO_2 minerals is that they commonly occur with incorporated Ca or other mono- or divalent cations. These are located in the “tunnels” of the tunnel-type minerals and between the layers of MnO_2 in other common mineral forms. The incorporated cations are typically non-stoichiometric, disordered and exchangeable with ions in an essentially aqueous environment. It is not difficult to imagine a scenario in which a cluster of four Mn and a Ca with associated oxygen atoms was captured from a medium from which these minerals were precipitating.

6.2. X-ray crystallography

A further criterion for narrowing the choice of favored cluster geometries comes from the X-ray crystallography of PS II [32,33]. Although the present structure is of limited resolution, it is possible to discern a cluster of four atoms attributable to Mn. The location of Ca relative to this cluster has not yet been reported. The arrangement of the Mn atoms has been described as pear-shaped (an elongated ellipsoid) with all four Mn lying approximately in the same plane. Among the clusters extracted from the mineral structures and having three

2.7-Å Mn–Mn vectors and one or two 3.3-Å Mn–Mn vectors, a single set of candidates also satisfies the PS II crystallographic criteria.

6.3. The present working model

The present preferred cluster model (see Fig. 2) was suggested among others in an earlier publication from our group (structure G in Fig. 9 of Ref. [1]) and is an example that is also preferred on the basis of EPR and ENDOR data [57,58]. Several geometric isomers of the model are possible, but they all satisfy the basic criteria. Three Mn atoms can be thought of as at the corners of the base of a trigonal pyramid, with an O atom at the apex and three additional O atoms forming bridges pairwise among the Mn atoms below the base. The fourth Mn is linked to one of the corner Mn atoms by a single O-atom bridge. Assuming that the bonding at each Mn is approximately octahedral, as in the minerals, there are isomers in which the link to the fourth Mn occurs through coordination directed above (toward the apical O) or below (away from the apical O) the plane of the other three Mn. Two chirally related isomers of the latter arrangement are possible. Rotation about a single O-atom bridge to the fourth Mn atom allows for this atom to be located close to the plane of the other three, even without taking into consideration distortions resulting from restrictions imposed by the local arrangement of ligands from the protein and associated water molecules. The studies of X-ray dichroism of single PS II crystals should help to refine this model and to place the Ca atom(s) relative to the Mn cluster.

It is worth noting in structure G (Fig. 2) that two of the Mn are topologically equivalent (apart from peripheral ligands from the protein matrix), whereas the corner atom that is linked to the fourth Mn and the fourth atom itself are topologically distinct. It has been proposed previously that the redox activity of the cluster may be associated primarily with only two of the Mn atoms—the others playing a role in stabilizing the structure and helping to provide the unique redox characteristics.

Fig. 2 (Fig. 10 of Ref. [31]) shows two additional structures, L and M, that may be considered to be modifications of G. The modifications can be simply described. We have pictured the arrangement of three of the Mn as the base corners of a trigonal pyramid with an O atom at the apex. There are three more O atoms bridging pairs of Mn on the opposite side of the plane of the Mn from the apical O. Of the three additional O atoms, two may be described as proximal and one distal to the Mn that is linked to the unique Mn. To obtain structure L from G, it is sufficient to move one of the proximal O atoms and use it to form the second leg of a di-μ-oxo bridge to the unique Mn atom. Similarly, structure M can be generated by removing the distal O to form the second leg of the bridge to the unique Mn. (As drawn in Fig. 10 [31], the four Mn atoms in structures L or M would not lie approximately in a plane. Agreement with the evidence from X-ray crystallography could be obtained, however, by moving one of the O atoms bridging to the unique Mn to the unoccupied coordination site of the Mn to which it is linked. These are simple structural isomers of those pictured for L and M.) If each Mn retains approximately octahedral coordination in structures L and M, however, there would now be four 2.7-Å Mn–Mn vectors and no 3.3-Å vectors. Some relaxation induced by the ligand environment around the cube corner could increase one of the 2.7-Å vector lengths, but stretching this to 3.3 Å would produce a significant distortion of the octahedral coordination geometries and perhaps introduce significant chemical strain. In our survey of the structures of manganese oxide minerals [34], the 3.3-Å vectors were always associated with planar (sp^2-type) O atom bridging, rather than the apical (sp^3-type) pictured in structures L and M. While we cannot rule out at present that substantial distortion occurs or that one or more of the Mn is 14 pentavalent, nevertheless we feel that structure G is the most reasonable one that is consistent with the experimental data.

7. Mechanism of water oxidation

Key steps in the oxidation of water to dioxygen include the removal of four H atoms from two water molecules and their release as H^+, transfer of four electrons to the electron transfer chain and to PS I, the formation of the O–O bond and the final oxidation and release of O_2. Relatively little is known about the nature of these steps in the overall water oxidation process, although considerable progress has been made in determining the steps where water binds to the oxygen evolving complex (OEC) [59,60].

7.1. Role of Ca^{2+} ion

The requirement for Ca^{2+} (or its replacement by Sr^{2+}) for O_2 evolution activity together with the demonstrated proximity of Ca to Mn in the cluster provides the basis for assigning it a role in the process. There is no way at present to know which Mn in the cluster are proximal to the essential Ca^{2+}, but presumably it is the Mn involved most intimately in the redox chemistry (Fig. 4). Ca^{2+} is a good electrophile, and its interaction with the oxygen of a water molecule should facilitate the release of protons [61]. If the deprotonated O is involved in bridging to Mn, it could subsequently begin to lose electrons to the transition-metal cluster as the latter becomes progressively more oxidized by the reaction center. Until more detailed structural information is available, this may be the limit of what we can say about the role of Ca^{2+} in this reaction.

7.2. Redox chemistry

Although the X-ray spectra are strongly supportive of Mn cluster oxidation during the $S_0 \rightarrow S_1$ and $S_1 \rightarrow S_2$ transitions, they do not support a similar Mn-centered oxidation during $S_2 \rightarrow S_3$. Furthermore, EXAFS analyses show clear evidence of non-degeneracy in the three 2.7-Å vector lengths in S_0 and S_3, but not in S_1 and S_2. These observations must be considered in any postulation of mechanistic aspects of the successive steps in water oxidation. Starting with S_0 and considering its role in the cyclic process, it immediately follows the release of O_2 and the reduction of the complex in preparation for its action on the next round of water. The conclusion that S_0 contains one Mn–Mn vector at 2.85 Å and two at 2.7 Å has been attributed to protonation of one of the proximal base oxygens, as indicated in Fig. 10 in Robblee et al. [31], and in a cluster where the oxidation state is $Mn_4(III_3,IV)$ in the S_0 state. Evidence from modelcompound studies shows that protonation of a bridging O results in lengthening of the di-μ-oxo bridged Mn–Mn vector. The transition $S_0 \rightarrow S_1$ changes the oxidation state to $Mn_4(III_2,IV_2)$ and decreases the 2.85-Å vector such that the lengths of the three are unresolvable in S_1. If our explanation of the unusual length in S_0 is correct, this implies that the proton is released from the bridging O atom during $S_0 \rightarrow S_1$. Whether this proton is transferred to an adjacent group or inserted into a hydrogen wire is unknowable at present. It may, however, reflect the first deprotonation step in the water-oxidation process.

During the $S_1 \rightarrow S_2$ transition, oxidation to the Mn_4 (III,IV_3) state occurs. This is the species that gives rise to the EPR multi-line signal. There is no significant evidence of accompanying structural changes. By contrast, the transition $S_2 \rightarrow S_3$ involves significant lengthening of probably all three (short) Mn–Mn vectors, and re-introduction of heterogeneity in the lengths [29]. At the same time, no clear evidence of Mn oxidation is seen [30]. This is unlikely to reflect simply a re-protonation of one or more of the O-atom bridges. The absence of Mn oxidation requires that something else has lost an electron during $S_2 \rightarrow S_3$. An obvious candidate is the involvement of one or more O atoms in the penultimate step prior to the release of O_2. For example, it has been proposed that Mn–Mn vector lengthening results from the removal of an electron from a bridging O atom to form an O**.** radical bridge [30]. The reason that all three vectors are lengthened may be that the

unpaired electron of the $O^{\cdot}$ radical is delocalized among the three bridges; their structural inequivalence would then account for the observed heterogeneity of Mn–Mn vector lengths in S_3.

No structural or spectroscopic evidence is available about the S4 state. It is known that there is a few milliseconds delay between the arrival of the last photon at the PS II reaction center and the detection of released O_2 [62]. Thus, there is time for significant chemical rearrangement of S_3, perhaps through one or more peroxo-type intermediates, and the attachment of substrate water for the next cycle of the process. The details of this part of the reaction await the isolation of intermediates or direct evidence of their presence in transient studies.

8. Conclusions

The essential nature of Mn, of Ca, of Cl and of the cluster geometry in the water oxidation process highlights the importance of obtaining high-resolution structural information from the ongoing X-ray crystallographic studies. Already these investigations, together with investigations of PS II mutants, have helped to develop a picture of the parts of the protein matrix, primarily but not exclusively the D1 polypeptide, that interact directly with the Mn cluster [63,64]. Among relatively few remaining candidates for the Mn cluster geometry that are consistent with available spectroscopic and structural evidence, the models presented in this paper (G and related structures in Fig. 2) are frontrunners. Furthermore, the spectroscopic evidence has provided insight into both redox and structural changes associated with individual S-state transitions. It is timely for synthetic inorganic chemists to use the biomimetic approach to produce a designer compound that exhibits water oxidation capability, and some very promising efforts by several groups are underway.

Acknowledgments

This work was supported by the Director, Office of Science, Office of Basic Energy Sciences, Division of Chemical Sciences, Geosciences, and Biosciences, US Department of Energy under contract DE-AC03-76SF00098, and by the National Institutes of Health grant (GM 55302). The important contributions to the research presented in this article by the many graduate students, postdoctoral fellows, and visiting scholars are gratefully acknowledged. We thank our collaborators Profs. K. Wieghardt, G. Christou, W.H. Armstrong, J.-J. Girerd and R.M. Mukherjee for generously providing all the inorganic Mn compounds. We thank Dr. Junko Yano for reading the manuscript and for her comments. Synchrotron radiation facilities were provided by the Stanford Synchrotron Radiation Laboratory (SSRL) and the Advanced Photon Source (APS), both supported by the US Department of Energy. The Biotechnology Laboratory at SSRL and BioCAT at the APS is supported by the National Center for Research Resources of the National Institutes of Health.

Abbreviations

EPR	electron paramagnetic resonance
EXAFS	extended X-ray absorption fine structure
MLS	multiline EPR signal
OEC	oxygen evolving complex
PS II	photosystem II
Y_D	tyrosine D
Y_Z	tyrosine Z
XANES	X-ray absorption near edge structure
XAS	X-ray absorption spectroscopy

XES X-ray emission spectroscopy

References

1. DeRose VJ, Mukerji I, Latimer MJ, Yachandra VK, Sauer K, Klein MP. Comparison of the manganese oxygen-evolving complex in photosystem II of spinach and *Synechococcus* sp. with multinuclear manganese model compounds by X-ray absorption spectroscopy. J. Am. Chem. Soc. 1994; 116:5239–5249.
2. Ke, B. Photosynthesis—Photobiochemistry and Photophysics. Vol. Vol. 10. Dordrecht, Netherlands: Kluwer Academic Publishers; 2001.
3. Clayton RK. Research on photosynthetic reaction centers from 1932 to 1987. Photosynth. Res. 2002; 73:63–71. [PubMed: 16245105]
4. Delosme R, Joliot P. Period four oscillations in chlorophyll a fluorescence. Photosynth. Res. 2002; 73:165–168. [PubMed: 16245118]
5. Commoner B, Heise JJ, Townsend J. Light-induced paramagnetism in chloroplasts. Proc. Natl. Acad. Sci. U. S. A. 1956; 42:710–718. [PubMed: 16589937]
6. Sogo PB, Pon NG, Calvin M. Photo spin resonance in chlorophyll-containing plant material. Proc. Natl. Acad. Sci. U. S. A. 1957; 43:387–393. [PubMed: 16590024]
7. Joliot P, Barbieri G, Chabaud R. A new model of the photochemical centers of system II. Photochem. Photobiol. 1969; 10:309–329.
8. Kok B, Forbush B, McGloin M. Cooperation of charges in photosynthetic oxygen evolution: I. A linear four step mechanism. Photochem. Photobiol. 1970; 11:457–475. [PubMed: 5456273]
9. Babcock, GT. PhD Dissertation. Berkeley: University California; 1973. Lawrence Berkeley Laboratory Report LBL-2172.
10. Babcock GT, Sauer K. Electron paramagnetic resonance signal II in spinach chloroplasts: I. Kinetic analysis for untreated chloroplasts. Biochim. Biophys. Acta. 1973; 325:483–503. [PubMed: 4360257]
11. Babcock GT, Sauer K. Electron paramagnetic resonance signal II in spinach chloroplasts: II. Alternative spectral forms and inhibitor effects on kinetics of signal II in flashing light. Biochim. Biophys. Acta. 1973; 325:504–519. [PubMed: 4360258]
12. Babcock GT, Sauer K. Rapid, light-induced transient in electron paramagnetic resonance signal II activated upon inhibition of photosynthetic oxygen evolution. Biochim. Biophys. Acta. 1975; 376:315–328. [PubMed: 163649]
13. Babcock GT, Sauer K. Rapid component of electron paramagnetic resonance signal II. Candidate for the physiological donor to photo-system II in spinach chloroplasts. Biochim. Biophys. Acta. 1975; 376:329–344. [PubMed: 163650]
14. Petrouleas V, Diner BA. Identification of Q_{400}, a high-potential electron-acceptor of photosystem-II, with the iron of the quinone–iron acceptor complex. Biochim. Biophys. Acta. 1986; 849:264–275.
15. Babcock GT, Sauer K. 2 electron donation sites for exogenous reductants in chloroplast photosystem-2. Biochim. Biophys. Acta. 1975; 396:48–62. [PubMed: 167849]
16. Boska M, Sauer K, Buttner W, Babcock GT. Similarity of electron-paramagnetic-resonance signal-IIf rise and $P680^+$ decay kinetics in tris-washed chloroplast photosystem-II preparations as a function of pH. Biochim. Biophys. Acta. 1983; 722:327–330.
17. Blankenship RE, Babcock GT, Sauer K. Kinetic study of oxygen evolution parameters in tris-washed, reactivated chloroplasts. Biochim. Biophys. Acta. 1975; 387:165–175. [PubMed: 164938]
18. Ley AC, Babcock GT, Sauer K. Flash kinetics and light intensity dependence of oxygen evolution in the blue-green alga *Anacystis nidulans*. Biochim. Biophys. Acta. 1975; 387:379–387. [PubMed: 804933]
19. Blankenship RE, Babcock GT, Warden JT, Sauer K. Observation of a new epr transient in chloroplasts that may reflect electron-donor to photosystem 2 at roomtemperature. FEBS Lett. 1975; 51:287–293. [PubMed: 164380]

20. Babcock GT, Blankenship RE, Sauer K. Reaction kinetics for positive charge accumulation on the water side of chloroplast photo-system II. FEBS Lett. 1976; 61:286–289. [PubMed: 174952]
21. Barry BA, Babcock GT. Tyrosine radicals are involved in the photosynthetic oxygen-evolving system. Proc. Natl. Acad. Sci. U. S. A. 1987; 84:7099–7103. [PubMed: 3313386]
22. Debus RJ, Barry BA, Babcock GT, McIntosh L. Site-directed mutagenesis identifies a tyrosine radical involved in the photosynthetic oxygen-evolving system. Proc. Natl. Acad. Sci. U. S. A. 1988; 85:427–430. [PubMed: 2829186]
23. Debus RJ, Barry BA, Sithole I, Babcock GT, McIntosh L. Directed mutagenesis indicates that the donor to $P680^+$ in photosystem II is tyrosine-161 of the D1 polypeptide. Biochemistry. 1988; 27:9071–9074. [PubMed: 3149511]
24. Rutherford, AW.; Zimmermann, J-L.; Boussac, A. The Photosystems: Structure. In: Barber, J., editor. Function, and Molecular Biology. Amsterdam: Elsevier; 1992. p. 179-229.
25. Debus RJ. The manganese and calcium ions of photosynthetic oxygen evolution. Biochim. Biophys. Acta. 1992; 1102:269–352. [PubMed: 1390827]
26. Yachandra VK, Sauer K, Klein MP. Manganese cluster in photosynthesis: where plants oxidize water to dioxygen. Chem. Rev. 1996; 96:2927–2950. [PubMed: 11848846]
27. Britt, RD. Oxygenic Photosynthesis: The Light Reactions. Ort, DR.; Yocum, CF., editors. Dordrecht: Kluwer Academic Publishers; 1996. p. 137-164.
28. Robblee JH, Cinco RM, Yachandra VK. X-ray spectroscopy based structure of the Mn cluster and mechanism of photosynthetic oxygen evolution. Biochim. Biophys. Acta. 2001; 1503:7–23. [PubMed: 11115621]
29. Liang W, Roelofs TA, Cinco RM, Rompel A, Latimer MJ, Yu WO, Sauer K, Klein MP, Yachandra VK. Structural change of the Mn cluster during the S2 to S3 state transition of the oxygen-evolving complex of photosystem: II. Does it reflect the onset of water/substrate oxidation? Determination by Mn X-ray absorption spectroscopy. J. Am. Chem. Soc. 2000; 122:3399–3412.
30. Messinger J, Robblee JH, Bergmann U, Fernandez C, Glatzel P, Visser H, Cinco RM, McFarlane KL, Bellacchio E, Pizarro SA, Cramer SP, Sauer K, Klein MP, Yachandra VK. Absence of Mn-centered oxidation in the S_2 to S_3 transition: implications for the mechanism of photosynthetic water oxidation. J. Am. Chem. Soc. 2001; 123:7804–7820. [PubMed: 11493054]
31. Robblee JH, Messinger J, Cinco RM, McFarlane KL, Fernandez C, Pizarro SA, Sauer K, Yachandra VK. The Mn cluster in the S_0 state of the oxygen-evolving complex of photosystem II studied by exafs spectroscopy: are there three di-μ-oxo-bridged Mn_2 moieties in the tetranuclear Mn complex? J. Am. Chem. Soc. 2002; 124:7459–7471. [PubMed: 12071755]
32. Zouni A, Wit H-T, Kern J, Fromme P, Krauβ N, Saenger W, Orth P. Crystal structure of photosystem II from *Synechococcus elongatus* at 3.8 Å resolution. Nature. 2001; 409:739–743. [PubMed: 11217865]
33. Kamiya N, Shen JR. Crystal structure of oxygen-evolving photo-system II from *Thermosynechococcus vulcanus* at 3.7-angstrom resolution. Proc. Natl. Acad. Sci. U. S. A. 2003; 100:98–103. [PubMed: 12518057]
34. Sauer K, Yachandra VK. A possible evolutionary origin for the Mn_4 cluster of the photosynthetic water oxidation complex from natural MnO_2 precipitates in the early ocean. Proc. Natl. Acad. Sci. U. S. A. 2002; 99:8631–8636. [PubMed: 12077302]
35. Dismukes GC, Siderer Y. Intermediates of a polynuclear manganese cluster involved in photosynthetic oxidation of water. Proc. Natl. Acad. Sci. U. S. A. 1981; 78:274–278. [PubMed: 16592949]
36. Hansson Ö, Andréasson LE. EPR-detectable magnetically interacting manganese ions in the photosynthetic oxygen-evolving system after continuous illumination. Biophys. Biochim. Acta. 1982; 679:261–268.
37. Kim DH, Britt RD, Klein MP, Sauer K. The g = 4.1 epr signal of the S_2 state of the photosynthetic oxygen-evolving complex arises from a multinuclear manganese cluster. J. Am. Chem. Soc. 1990; 112:9389–9391.
38. Peloquin JM, Britt RD. EPR/ENDOR characterization of the physical and electronic structure of the OEC Mn cluster. Biochim. Biophys. Acta. 2001; 1503:96–111. [PubMed: 11115627]

39. Messinger J, Robblee J, Yu WO, Sauer K, Yachandra VK, Klein MP. The S_0 state of the oxygen-evolving complex in photosystem II is paramagnetic: detection of an epr multiline signal. J. Am. Chem. Soc. 1997; 119:11349–11350.
40. Ahrling KA, Peterson S, Styring S. An oscillating manganese electron paramagnetic resonance signal from the S_0 state of the oxygen evolving complex in photosystem II. Biochemistry. 1997; 36:13148–13152. [PubMed: 9376375]
41. Dexheimer SL, Klein MP. Detection of a paramagnetic intermediate in the S_1 state of the photosynthetic oxygen-evolving complex. J. Am. Chem. Soc. 1992; 114:2821–2826.
42. Campbell KA, Peloquin JM, Pham DP, Debus RJ, Britt RD. Parallel polarization epr detection of an S_1-state multiline epr signal in photosystem II particles from *Synechocystis* sp. Pcc 6803. J. Am. Chem. Soc. 1998; 120:447–448.
43. Boussac A, Zimmermann J-L, Rutherford AW. EPR signals from modified charge accumulation states of the oxygen evolving enzyme in Ca^{2+}-deficient photosystem II. Biochemistry. 1989; 28:8984–8989. [PubMed: 2557913]
44. Sivaraja M, Tso J, Dismukes GC. A calcium-specific site influences the structure and activity of the manganese cluster responsible for photosynthetic water oxidation. Biochemistry. 1989; 28:9459–9464. [PubMed: 2558720]
45. Matsukawa T, Mino H, Yoneda D, Kawamori A. Dual-mode epr study of new signals from the S_3-state of oxygen-evolving complex in photosystem II. Biochemistry. 1999; 38:4072–4077. [PubMed: 10194321]
46. Blankenship R, McGuire A, Sauer K. Chemically induced dynamic electron polarization in chloroplasts at room-temperature— evidence for triplet-state participation in photosynthesis. Proc. Natl. Acad. Sci. U. S. A. 1975; 72:4943–4947. [PubMed: 174083]
47. Rutherford AW. Orientation of epr signals arising from components in photosystem II membranes. Biochim. Biophys. Acta. 1985; 807:189–201.
48. Jaklevic J, Kirby JA, Klein MP, Robertson AS, Brown GS, Eisenberger P. Fluorescence detection of exafs: sensitivity enhancement for dilute species and thin films. Solid State Commun. 1977; 23:679–682.
49. Roelofs TA, Liang W, Latimer MJ, Cinco RM, Rompel A, Andrews JC, Sauer K, Yachandra VK, Klein M. Oxidation states of the manganese cluster during the flash-induced s-state cycle of the photosynthetic oxygen-evolving complex. Proc. Natl. Acad. Sci. U. S. A. 1996; 93:3335–3340. [PubMed: 11607649]
50. Latimer MJ, DeRose VJ, Mukerji I, Yachandra VK, Sauer K, Klein MP. Evidence for the proximity of calcium to the manganese cluster of photosystem II: determination by X-ray absorption spectroscopy. Biochemistry. 1995; 34:10898–10909. [PubMed: 7662671]
51. Cinco RM, Holman KLM, Robblee JH, Yano J, Pizarro SA, Bellacchio E, Sauer K, Yachandra VK. Calcium exafs establishes the Mn–Ca cluster in the oxygen-evolving complex of photosystem II. Biochemistry. 2002; 41:12928–12933. [PubMed: 12390018]
52. Mukerji I, Andrews JC, DeRose VJ, Latimer MJ, Yachandra VK, Sauer K, Klein MP. Orientation of the oxygen-evolving manganese complex in a photosystem II membrane preparation: an X-ray absorption spectroscopy study. Biochemistry. 1994; 33:9712–9721. [PubMed: 8068650]
53. Cinco RM, Robblee JH, Rompel A, Fernandez C, Sauer K, Yachandra VK, Klein MP. Proximity of calcium to the manganese cluster of the photosynthetic oxygen-evolving complex determined from strontium xafs. J. Synchrotron Radiat. 1999; 6:419–420. [PubMed: 15263329]
54. Brudvig GW, Crabtree RH. Mechanism for photosynthetic oxygen evolution. Proc. Natl. Acad. Sci. U. S. A. 1986; 83:4586–4588. [PubMed: 3460059]
55. Sauer, K.; Yachandra, VK.; Britt, RD.; Klein, MP. Manganese Redox Enzymes. Pecoraro, VL., editor. New York: VCH Publishers; 1992. p. 141-175.
56. Russell, MJ.; Hall, AJ. Sixth International Congress on Carbon Dioxide Utilization. Breckinridge, CO: 2001. p. 49
57. Peloquin JM, Campbell KA, Randall DW, Evanchik MA, Pecoraro VL, Armstrong WH, Britt RD. ^{55}Mn endor of the S_2-state multiline epr signal of photosystem II: implications on the structure of the tetranuclear cluster. J. Am. Chem. Soc. 2000; 122:10926–10942.

58. Hasegawa K, Ono T-A, Inoue Y, Kusunoki M. Spin-exchange interactions in the S_2-state manganese tetramer in photosynthetic oxygen-evolving complex deduced from g = 2 multiline epr signal. Chem. Phys. Lett. 1999; 300:9–19.

59. Messinger J, Badger M, Wydrzynski T. Detection of *one* slowly exchanging substrate water molecule in the S_3 state of photosystem II. Proc. Natl. Acad. Sci. U. S. A. 1995; 92:3209–3213. [PubMed: 11607525]

60. Messinger J. Towards understanding the chemistry of photosynthetic oxygen evolution: dynamic structural changes, redox states and substrate water binding of the Mn cluster in photosystem II. Biochim. Biophys. Acta. 2000; 1459:481–488. [PubMed: 11004466]

61. Vrettos JS, Stone DA, Brudvig GW. Quantifying the ion selectivity of the Ca^{2+} site in photosystem II: evidence for direct involvement of Ca^{2+} in O_2 formation. Biochemistry. 2001; 40:7937–7945. [PubMed: 11425322]

62. Joliot P, Hoffnung M, Chabaud R. Study of the evolution of oxygen by algae illuminated by sinusoidally modulated light. J. Chim. Phys. 1966; 63:1423–1441.

63. Debus RJ. Amino acid residues that modulate the properties of tyrosine Yz and the manganese cluster in the water oxidizing complex of photosystem II. Biochim. Biophys. Acta. 2001; 1503:164–186. [PubMed: 11115632]

64. Diner BA. Amino acid residues involved in the coordination and assembly of the manganese cluster of photosystem II. Proton-coupled electron transport of the redox-active tyrosines and its relationship to water oxidation. Biochim. Biophys. Acta. 2001; 1503:147–163. [PubMed: 11115631]

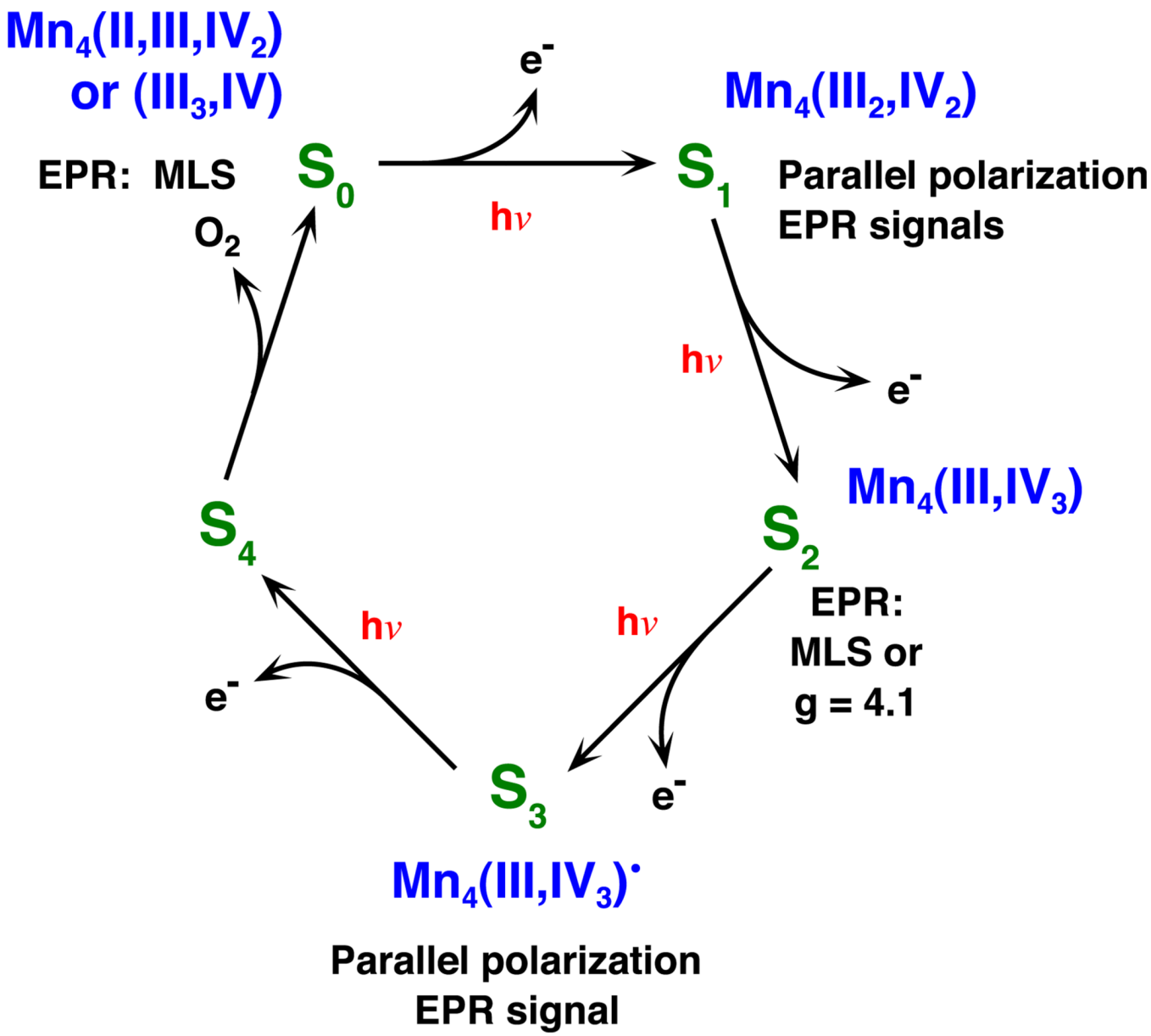

Fig. 1.
The Kok S-state scheme with the oxidation state assignments of the tetranuclear Mn complex derived from our XANES and XES studies [30,49], and EPR spectroscopy. The EPR signals identified with the particular S-states are also indicated.

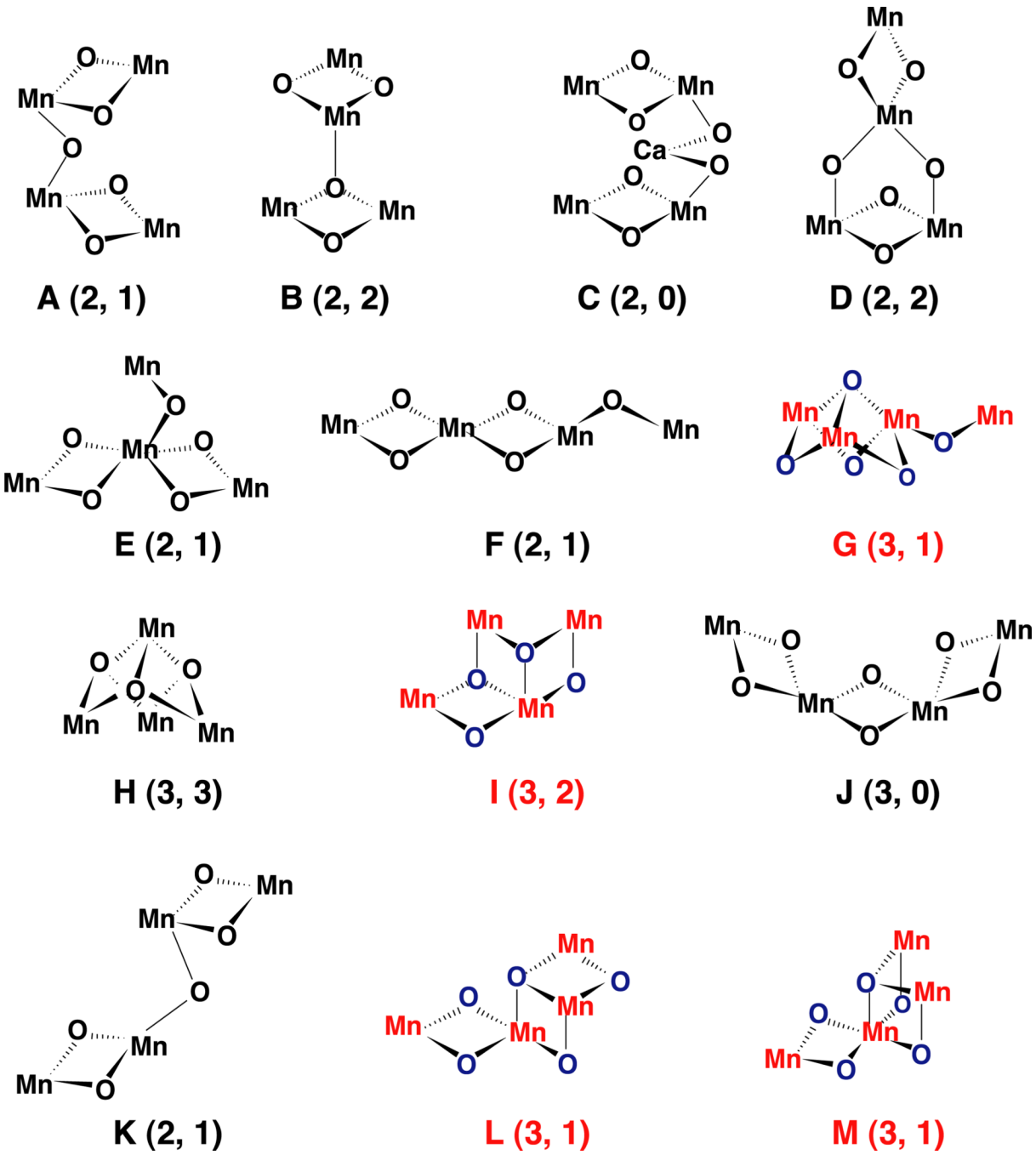

Fig. 2.

Topological models for the Mn complex identified as compatible with the EXAFS data by DeRose et al. [1] and Robblee at al. [31]. The nomenclature is identical to the one we have used in our two earlier publications by DeRose et al. and Robblee et al. The numbers in parenthesis are the number of short 2.7- to 2.8-Å Mn–Mn vectors and long 3.3- to 3.4-Å Mn–Mn vectors. The topologies in color (options G, I, L and M) all have three short 2.7- to 2.8-Å Mn–Mn vectors and are in better agreement with the X-ray diffraction studies; options E, F and G have been identified as compatible with EPR and ENDOR data. Option G or a topological isomer seems to be the best model by all presently available criteria (X-ray diffraction, EXAFS and EPR).

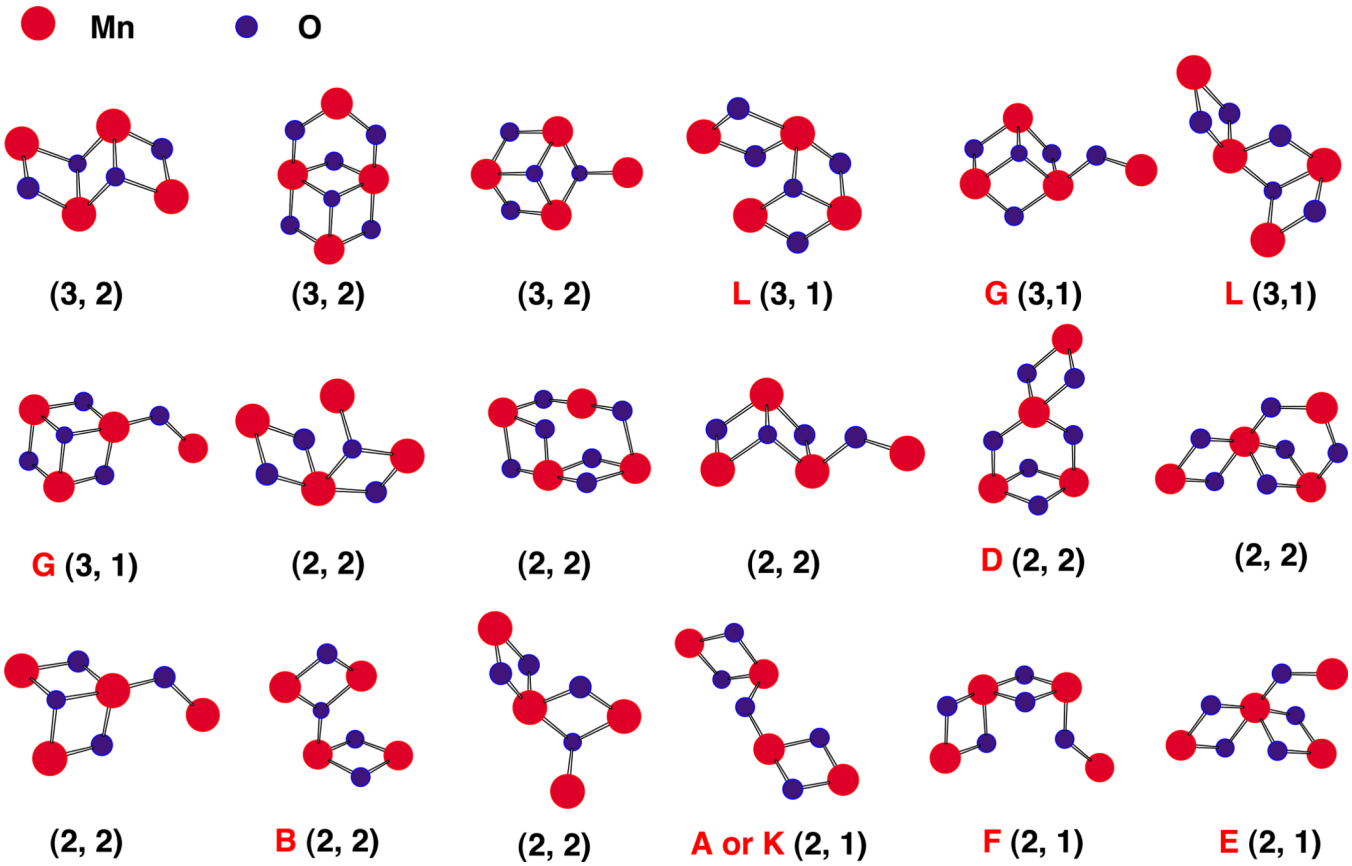

Fig. 3.

Some possible Mn4 clusters and oxygens extracted from the hollandite lattice in categories that are compatible with that associated with the OEC. Structures are organized according to *m*, the number of 2.7– 2.8-Å Mn–Mn vectors and *n*, the number of 3.3–3.4-Å vectors, and given the designation (*m*, *n*). Mn atoms are in red and only the bridging O atoms (in blue) are shown. Some of the motifs identified in these tunnel-like minerals were previously proposed to be compatible with the EXAFS data from the OEC; they are identified by the alphabet according to DeRose et al. [1] and Robblee et al. [31]; others are an entirely new class of topological alternatives that need to be explored as candidates for the OEC. Adapted from Sauer and Yachandra [34].

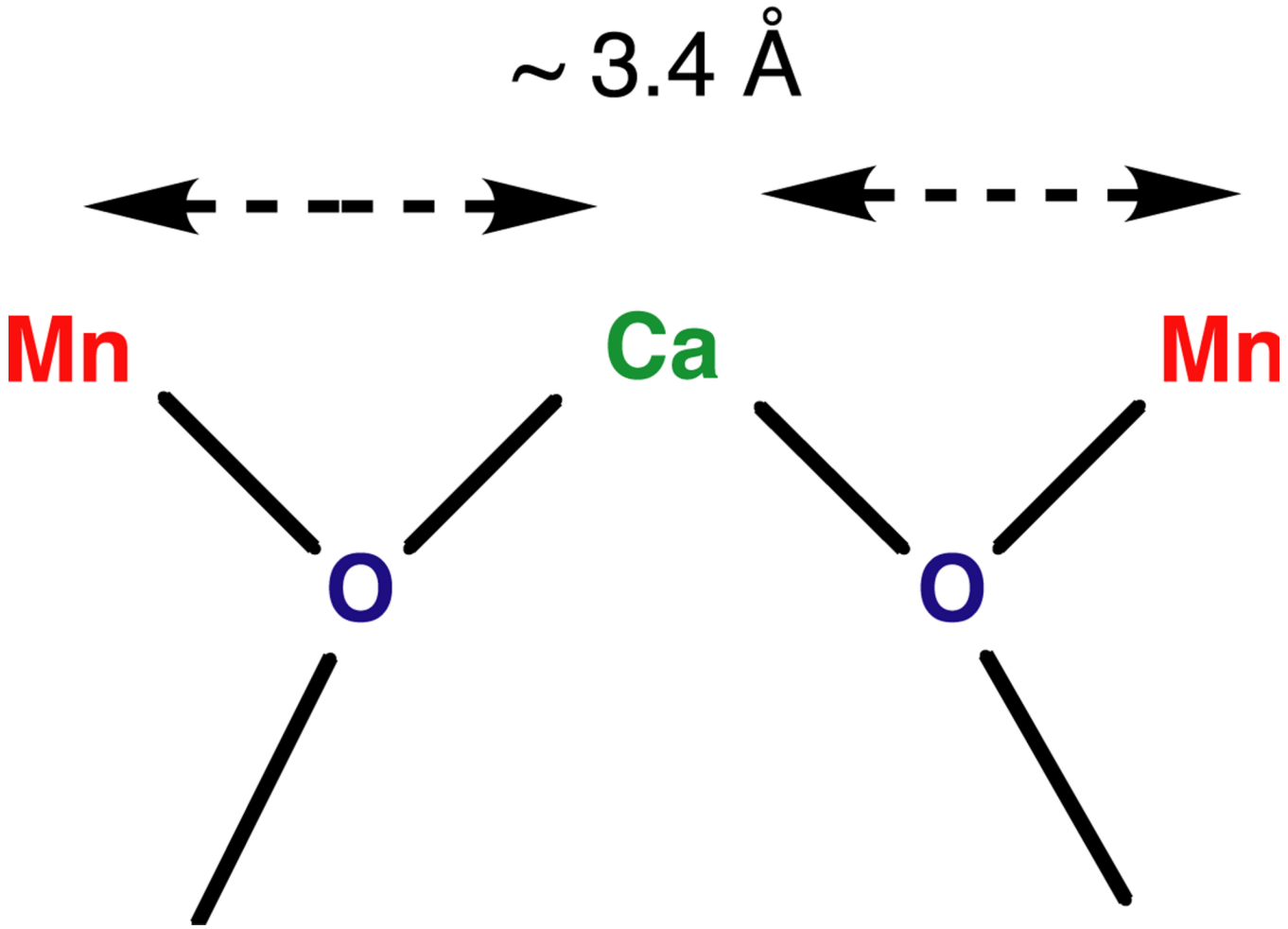

Fig. 4.

Model of Ca-binding site of the oxygen-evolving complex in PS II. From the results of the Ca EXAFS studies on PS II, the Ca cofactor is linked by two single-O bridges to two Mn. The oxygens can be provided by water, hydroxyl or protein residues (carboxylate, phenolate). Other ligands to Ca are not shown. The arrangement shown here is not unique, because other placements of the two Mn around the Ca are conceivable. Adapted from Cinco et al. [51].